Chemical Engineering Journal 102 (2004) 11–24

Chemical Engineering Journal

www.elsevier.com/locate/cej

Pressure drops of single and two-phase flows through T-type microchannel mixers

Jun Yue, Guangwen Chen*, Quan Yuan

Dalian Institute of Chemical Physics, Chinese Academy of Sciences, Group 903, 457 Zhongshan Road, Dalian 116023, China

Received 14 November 2003; received in revised form 20 January 2004; accepted 5 February 2004

Abstract

In this paper, preliminary experimental results are presented on pressure drop characteristics of single and two-phase flows through two T-type rectangular microchannel mixers with hydraulic diameters of 528 and 333 μm, respectively. It is shown that both N_2 and water single-phase laminar flows in microchannels, with consideration of experimental uncertainties, are consistent with classic theory, if additional effects, such as entrance effects that will interfere with the interpretation of experimental results, are eliminated by carefully designing the experiments. The obtained pressure drop data of N_2–water two-phase flow in micromixers are analyzed and compared with existing flow pattern-independent models. It is found that the Lockhart–Martinelli method generally underpredicts the frictional pressure drop. Thereafter, a modified correlation of C value in the Chisholm's equation based on linear regression of experimental data is proposed to provide a better prediction of the two-phase frictional pressure drop. Also among the homogeneous flow models investigated, the viscosity correlation of McAdams indicates the best performance in correlating the frictional pressure drop data (mean deviations within ±20% for two micromixers both). Finally it is suggested that systematic studies are still required to accurately predict two-phase frictional performance in microchannels.

Keywords: Microchannel; Micromixer; Two-phase flow; Laminar flow; Pressure drop

1. Introduction

Rapid progresses in microelectromechanical systems (MEMS) and miniaturization technologies are bringing significant changes to chemical process engineering. By means of these technologies, we can build microstructured devices to intensify mixing, heat and mass transfer, and also reactions in chemical processes. Some successful efforts have already been reported in recent years [1–3]. Nevertheless, the fundamentals of transport phenomena and reactions occurring in such microchannel devices are still unclear, making it difficult to predict the performance of these devices precisely and quantitatively. Among these issues waiting to be addressed, single and two-phase flow behaviors in microchannels have the priority for the investigation, since these are crucial for successful designs and applications of microreaction technologies, e.g., gas–liquid microreactors [4,5], single and two-phase flow microchannel heat sinks [6,7], etc.

1.1. Single-phase flow in microchannels

For gas and liquid single-phase flows in microchannels, contradictory experimental and simulation results exist [8–25]. From the viewpoints of actual applications of microchannel reactors, we are mainly interested in fluid laminar flow behavior in microchannels with diameters of several hundred micrometers (termed "large microchannels" in the following paragraphs), where compressible effects and rarefaction effects are thought to be negligible.

Currently available research papers on fluid laminar flow in large microchannels reveal that the conclusions can be mainly classified into three categories (divided by the relationship between fRe and C): (1) $fRe > C$, i.e., fluid laminar flow in microchannels exhibits a higher pressure drop [8–16]; (2) $fRe < C$, i.e., the pressure drop of fluid laminar flow in microchannels is less than that predicted by classic theory [17,18]; and (3) $fRe = C$, i.e., fluid laminar flow in microchannels is still consistent with classic theory [19–25]. More details are tabulated in Table 1. Here fRe represents the product of friction factor, f, with Reynolds number, Re, and C is laminar friction constant according to classic theory for a specific geometrical microchannel.

* Corresponding author. Tel.: +86-411-437-9031; fax: +86-411-469-1570.
E-mail address: gwchen@dicp.ac.cn (G. Chen).

1385-8947/$ – see front matter © 2004 Elsevier B.V. All rights reserved.
doi:10.1016/j.cej.2004.02.001

Nomenclature

C	friction constant or coefficient in the Chisholm's equation
C_0	distribution parameter
D_H	hydraulic diameter (m)
f	Darcy friction factor
G	mass velocity (kg m^{-2} s^{-1})
H	height of the microchannel (m)
j	mixture volumetric flux (m s^{-1})
j_G	gas superficial velocity (m s^{-1})
j_L	liquid superficial velocity (m s^{-1})
L_e	entrance length (m)
ΔL	the length of pressure drop measurement (m)
Q	volumetric flow rate (m^3 s^{-1})
Δp	single-phase pressure drop (Pa)
Δp_A	acceleration pressure drop (Pa)
Δp_F	two-phase frictional pressure drop (Pa)
Δp_T	two-phase total pressure drop (Pa)
Re	Reynolds number
Re_{GS}	gas superficial Reynolds number
Re_{LO}	Reynolds number for liquid flowing at the two-phase mass velocity
Re_{LS}	liquid superficial Reynolds number
U	flow velocity (m s^{-1})
V_b	drift velocity (m s^{-1})
W	width of the microchannel (m)
We_{GS}	gas superficial Weber number
We_{LS}	liquid superficial Weber number
x	mass quality
X	Martinelli parameter

Subscripts

G	gas
L	liquid
TP	two-phase mixture

Greek symbols

α	aspect ratio or void fraction
β	volumetric quality
δX	uncertainty of variance X
μ	viscosity (Pa s)
ρ	density (kg m^{-3})
Φ_L^2	two-phase frictional multiplier

From Table 1, it can be seen that while there may be strong theoretical evidences supporting higher laminar flow friction constant in microchannels, articles reporting lower *fRe* (especially for liquids) are rare and lack reasonable arguments. However, when the tube diameter approaches micron scale, cautions must be taken to interpret the experimental results [26,27], where we think the measurement uncertainty of the microchannel size and entrance effects are two vital factors. As described by Judy et al. [23], and Liu and Garimella [24], the experimental results were still consistent with classic theory if entrance effects and measurement errors were considered.

1.2. Two-phase flow in microchannels

When two phases are confined in microchannels, the system will take on complex fluidic behaviors. As the channel diameter becomes smaller, the predominance of surface forces (surface tension etc.) will cause gas–liquid two-phase flow in microchannels to behave very differently from that in conventional large-sized tubes (>10 mm). For example, phenomena such as the disappearance of stratified flow regime, suppression of the bubbly flow existence region and flow characteristics independent of channel orientation will be expected for two-phase flow in microchannels [28–32].

Most currently available articles deal with two-phase flow in minichannels with diameters at the order of millimeters, and there have been very few papers until recently [28–32] concerning gas–liquid two-phase flow in microchannels having hydraulic diameters of several hundred micrometers or even smaller than 100 μm. However, since there is no strict size definition of a microchannel, those papers concerning channels with sizes approximating 1 mm are also referenced here as useful materials [33–37].

Previous studies have indicated that flow patterns and their transitions, void fraction and pressure drop characteristics of gas–liquid two-phase flow in microchannels are different from those in macrochannels. For comparatively large microchannels, significant changes in flow patterns have already been proven by several authors, for example, capillary bubbly flow [28] and bubble-train slug flow [33] were found to exist while horizontal stratified flow was missing [33,34]. It is noteworthy that flow patterns showed even more complicated structures in ultra small circular microchannels (≤100 μm). For an instance, in Serizawa et al.'s paper [29], a bubbly flow pattern with bubble size much smaller than the tube diameter (100 μm) was never observed and different flow patterns in the channel simultaneously occurred under given flow conditions; Kawahara et al. [30] confirmed that the wettability of the tube more obviously affected the two-phase flow structure. In addition, the relevant flow regime transition models and correlations so far were in poor agreement with the experimental data [28,34]. Therefore, in face of the above-mentioned difficulties and confusions in predictions of flow patterns and their transitions in microchannels, Akbar et al. [31] proposed a Weber number based flow pattern map and found that the available data for near-circular microchannels and air–water like fluid pairs were in reasonable agreement with the predictions by this map.

Even less satisfactory results existed for void fraction and pressure drop data of gas–liquid two-phase flow in microchannels. Triplett et al. [34] showed that the homogenous flow model had provided the best prediction of their experimental void fraction in bubbly flow and slug flow, and that the two-phase pressure drop was in good agree-

Table 1
Comparisons on results of current papers concerning fluid laminar flow in large microchannels

Reference	Microchannel specification	Fluid	Conclusion	Explanation
Wu and Little [8]	Silicon or glass substrate, trapezoidal or near trapezoidal, D_H: 45.46–83.08 μm	N_2, H_2, Ar	Much higher *fRe* value under laminar flow; early transition to turbulence, sometimes at *Re* as low as 400	Surface roughness effects; uncertainty in channel depth after bonding
Papautsky et al. [9]	Nickel electroformed microchannels, rectangular, width: 50–600 μm, depth: 20–30 μm	Water	*fRe* approximately 12% higher than that of macro-scale laminar flow predictions	Micropolar fluid theory
Pfund et al. [10]	Sandwich structure, rectangular, D_H: 128–521 μm, low aspect ratio	Water	*fRe* greater than the classic values in most cases; transitional Reynolds number lower than that for macroscopic ducts, but much larger than the values of 400–700	Roughness effects; measurement uncertainty
Ren et al. [11]*	Two parallel plates with height 14.1, 28.2 and 40.5 μm, respectively	Water, aqueous KCl solutions (10^{-4} and 10^{-2} M)	Up to 20% higher flow resistance for pure water and the low ionic concentration solution for the smallest microchannel	Electro-viscous effects
Mala and Li [15]	Fused silica and stainless steel, circular, D_H: 50–254 μm	Water	The deviation from the conventional theory occurred when Reynolds number was not very small and increased with decreasing diameter; material dependence of flow behavior	Roughness-viscosity model
Qu et al. [16]	Silicon, trapezoidal, D_H: 51.3–168.9 μm	Water	Pressure gradient and flow friction higher than that predicted by the conventional laminar flow theory	Roughness-viscosity model
Yu et al. [17]	Circular, D_H = 19, 52, 102 μm	N_2, water	$fRe = 53$ instead of 64	Not given
Jiang et al. [18]	Silicon, trapezoidal, D_H: 16.3–53.2 μm	Water	$fRe < 64$, *fRe* depended not only on cross-section sizes but also on the length of the microchannels	Not given
Flockhart and Dhariwal [19]	Silicon, trapezoidal, D_H: 50–120 μm	Water	Laminar flow results conform to macro scale laws	Good agreement with classic theory
Sharp et al. [20]	Polyimide-coated fuse silica capillary, D_H: 50–242 μm	Water, glycerol, 1-propanol	Flow in microtubes obeys classic laminar flow theory very well up to *Re* of 1100–1500	Ditto
Xu et al. [21]	Aluminum or silicon, rectangular, D_H: 30–344 μm	Water	Laminar flow characteristics in microchannels agree with conventional behaviors predicted by the Navier–Stokes equations	Ditto
Bau and Pfahler [22]	Silicon, trapezoidal, depth: 0.5–200 μm	Isopropyl alchol, silicone oil, water	The deviation of measured *fRe* from theoretical predictions are relatively small, within 20%	Ditto
Judy et al. [23]	Fused silica or stainless steel, circular or rectangular, D_H: 15–150 μm	Methanol, water, isopropanol	*fRe* data revealed no distinguishable deviation from macroscale stokes flow theory at $Re < 2000$	Ditto
Liu and Garimella [24]	Plexiglass, rectangular, D_H: 244–974 μm	Water	The experimental results agree closely with the theoretical predictions in the laminar region ($Re < 2000$)	Ditto
Wu and Cheng [25]	Silicon, smooth, trapezoidal or triangular, D_H: 25.9–291.0 μm	Water	The friction factors agree within ±11% of the analytical solution based on the Stokes flow theory; transition to turbulent flow at $Re \approx 1500$–2000 for large microchannels	Ditto

* Similar results can also be seen in other papers [12–14].

ment with the homogeneous mixture assumption based on McAdams correlation. However, for annular flow, all existing models over-predicted void fraction and pressure drop data. Zhao and Bi [32] suggested that the frictional pressure drop of air–water two-phase flow in triangular microchannels ($D_H = 866$ μm) could be well predicted by the Lockhart–Martinelli correlation if the newly proposed friction factor correlation for single-phase flow was adopted, and that the void fraction in slug flow could be well correlated by the drift-flux model with zero drift velocity. In

contrast, Kawahara et al. [30] achieved a much smaller void fraction value and concluded that the two-phase frictional pressure drop was over-predicted by the homogeneous flow models except Dukler et al.'s model for the mixture viscosity (within ±20% mean deviation) and that the two-phase friction multiplier values were correlated well (within ±10% mean deviation) with the separated flow model of Lockhart and Martinelli if the coefficient used in the Chisholm's equation, C, was assumed to be 0.24.

The above literature review shows that there are still relatively few experimental data available concerning two-phase flow of air–water like fluid pairs in circular or near circular microchannels (e.g., rectangular microchannels with aspect ratios approximating 1). Consequently, more experiments and theoretical analyses are required to clarify the difference of two-phase flow behaviors in microchannels from those in macrochannels.

Thus, the work of this paper is to present experimental results on pressure drops of single and two-phase flows through rectangular microchannels in T-type micromixers having hydraulic diameters of 528 and 333 μm, respectively. Further, the validity of classic laminar flow theory will be examined and existing empirical or semi-empirical flow pattern-independent models will be employed to explain the experimental two-phase results. Also some modifications for improving these models will be proposed, which may be expected to provide powerful support for further studies.

2. Experimental

2.1. T-type micromixer specification

The microchannel structures of a T-type micromixer were fabricated on a smooth polymethyl methacrylate (PMMA) substrate using conventional precision machining technology. Fig. 1 shows the geometric diagram of a T-type micromixer plate that has two inlet channels and one mixing channel. All channels built in the T-type micromixer plate were designed to have the same widths and depths. In the present experiments, two sized T-type micromixers were used, i.e., with microchannels having nominal hydraulic diameters of 500 and 300 μm, respectively. In the mixing channel, Sections 1–4, two pressure taps were located in positions 2 and 3 where two holes of 0.2 mm diameter were drilled at the bottom of the microchannel for the access of pressure measurement tubings. Also three holes of 3 mm diameter were drilled through the micromixer plate at the end of the inlet and outlet ports as connections to outer fluid conveying tubings on the backside.

In order to seal the micromixer plate before use, it was covered with a piece of transparent adhesive tape with one side towards the microchannel having adhesive. Then a smooth PMMA plate having the same outer dimension as the micromixer plate was placed on the top. Finally the three sections were clamped together tightly using screw

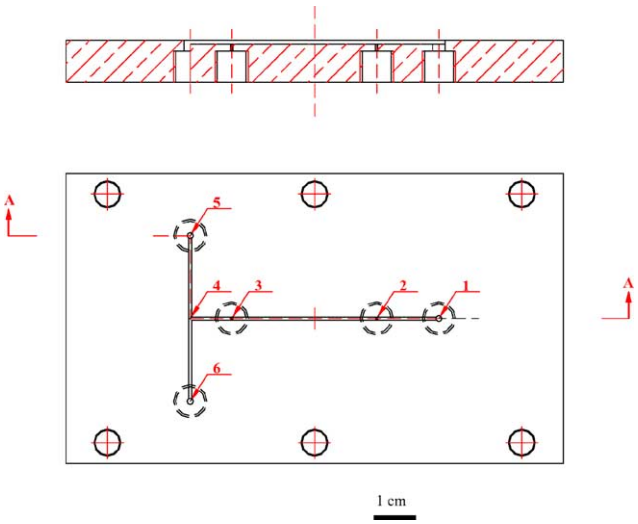

Fig. 1. Schematic of the T-type micromixer plate (the microchannel dimension is not in scale).

fittings through six bolting holes distributing symmetrically on the peripheries of the two PMMA plates, thus forming a T-type micromixer. Then necessary tubings were directly connected to the micromixer itself through connectors on the backside of the micromixer plate. Also gas tightness was checked to ensure that T-type micromixers were leakproof under static pressure of 0.3 MPa. A picture of the whole micromixer assembly is shown in Fig. 2. Thus, according to the present sealing method, the adhesive tape formed one wall of the microchannel whose property (hydrophobicity, etc.) might be slightly different from the other three walls. However, we think that this configuration is frequently met in microchannel applications (e.g., microchannels formed in the silicon wafer via anodic bond onto the Pyrex wafer [5]) and will not cause significant changes in overall two-phase pressure drop characteristics.

After single and two-phase flow experiments, the two micromixers were cut into four pieces along the mixing channel and were then made smooth, washed and dried. A microscope with micron scales in the X and Y-axes on the base was used to measure the cross-sectional sizes of the

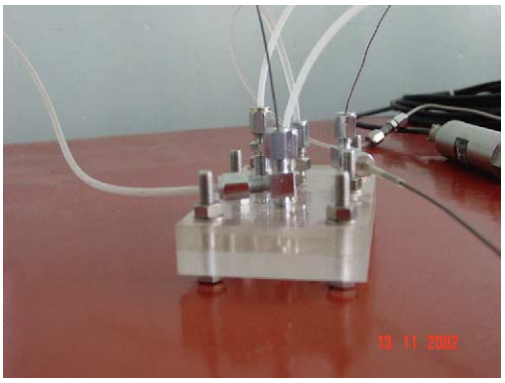

Fig. 2. Photograph of the whole T-type micromixer assembly.

Table 2
Specifications of the two T-type micromixers

Number	Nominal hydraulic diameter (μm)	H (μm)	W (μm)	D_H (μm)	Aspect ratio	Sectional distance (cm)				
						1–2	2–3	3–4	4–5	4–6
1	500	488	575	528	0.848	1.472	3.430	0.942	1.976	1.976
2	300	332	333	333	0.997	1.454	3.452	0.950	1.976	1.976

microchannels. Each piece was measured 3 or more times and results for multiple measurements were averaged together to give the final depths and widths of the microchannels in the mixing section for the two micromixers. It was found that changes in the microchannel size along the mixing channel were insignificant, generally within the measurement error. Typical microchannel cross-sectional images are shown in Fig. 3 and the detailed specifications of these two T-type micromixers are listed in Table 2. The cross-sectional sizes of two inlet channels were not measured and were thought to be identical to that of the mixing channel.

2.2. Experimental setup

The schematics of the test facilities for single and two-phase flow pressure drop measurements are clearly demonstrated in Fig. 4.

For single-phase flow test, experiments were performed for both N_2 and deionized water laminar flows in microchannels. In the former case, N_2 from the gas cylinder was conveyed by a pressure-regulating valve and was forced to flow through a filter to remove possible contaminations. Then a mass flow controller with range of 0–500 standard cubic centimeters per minute (SCCM) served to adjust its flow rate before it was introduced into port 1 (see Fig. 1) in the T-type micromixer. After horizontally flowing along the mixing channel in the 1–4 direction, N_2 was then divided into two streams and finally exited at the outlet ports 5 and 6. Two thermocouples (K-type) were located in the inlet port 1 and outlet port 6 to measure the corresponding

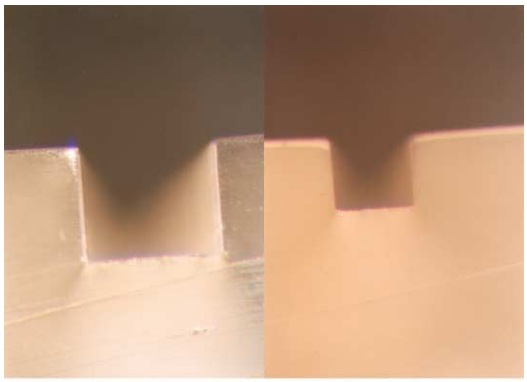

Fig. 3. Images of microchannels in the mixing sections of T-type micromixers: (a) $D_H = 528\,\mu m$; (b) $D_H = 333\,\mu m$.

temperatures of N_2 flowing in microchannels. A pressure transducer with range of 0–100 kPa was located at port 2 measuring the corresponding static pressure. The pressure drop between ports 2 and 3 was read directly from a U-tube manometer with water as the indicator at lower pressure drops (<6 kPa) and by the difference between two pressure transducers with ranges of 0–100 kPa located at ports 2 and 3 at higher pressure drops (≥6 kPa). In the experiments for deionized water flow, its flow rate was controlled by a 0–30 ml/min positive displacement pump. A filter was installed midway between the water reservoir and the pump to remove possible entrained particles and a buffer tank just after the pump was used to stabilize the flow rate. The flow route in the micromixer was the same as that for N_2 flow experiments. The water flow rate was also measured by an electronic balance (i.e., weighing the accumulated water in a container over a period of time, then calculating its flow rate). It was found that the measured water flow rate was in good linear relationship with the set value of the pump. For pressure difference measurement between ports 2 and 3, a U-tube manometer with CCl_4 as the indicator was applied for the micromixer with 528 μm hydraulic diameter while two different pressure transducers with ranges of 0–100 kPa were directly used for the micromixer with 333 μm hydraulic diameter.

For horizontal two-phase flow test, N_2 and boiled deionized water were regulated by the mass flow controller and the positive displacement pump mentioned above, respectively, as sketched in Fig. 4c. N_2 was flowing through one inlet channel, i.e., port 6 in the micromixer plate while water was entering from the other inlet channel (port 5). Subsequently they met at the beginning of the mixing channel and the resulting two-phase mixture was guided to flow along the 4–1 direction. After the two-phase mixture left the micromixer from the outlet port 1, it was discharged into air through a connecting tube. Static pressures at ports 2 and 3 were measured using two pressure transducers, with range of 0–100 kPa for lower static pressure and 0–1000 kPa for higher one. The inlet and outlet temperatures of the two phases were measured using three thermocouples (K-type). It should be noted that before each run during the two-phase flow experiments, water must be filled into the micromixer to remove any possible air remaining in it as well as the associated measuring and connecting systems.

Data on single and two-phase flow experiments were all recorded under steady-state conditions in order to reduce possible perturbation caused by the placement of two

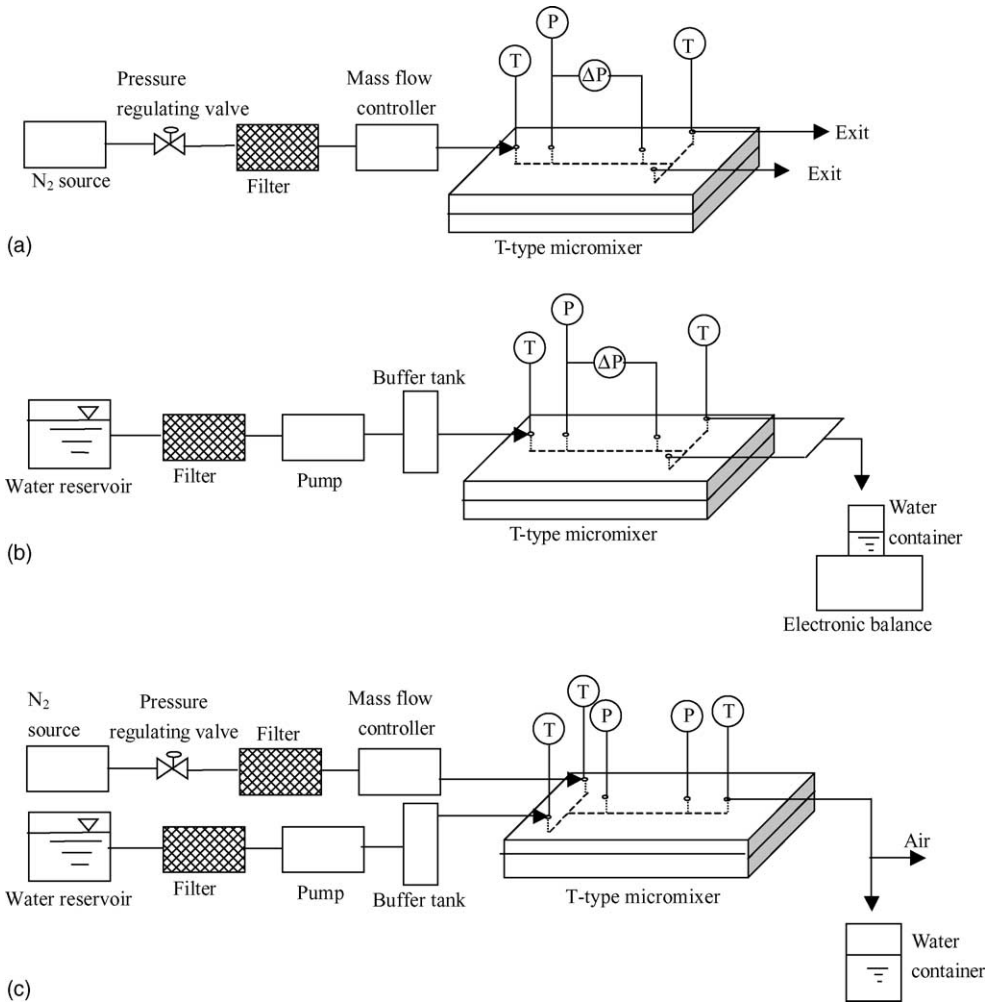

Fig. 4. Schematics of the test facilities: (a) N_2 single-phase flow; (b) water single-phase flow; (c) N_2–water two-phase flow.

pressure taps on board and it was found that this arrangement could always produce reliable and reproducible results.

3. Results and discussions

3.1. Single-phase flow

In the present single-phase flow experiments in microchannels, it was observed that in every run, the inlet and outlet fluid temperatures were very close to room temperature (293 K), so the experiments were thought to be conducted isothermally. Also due to the short distance between two pressure taps, the measured pressure drop was rather small compared to the absolute pressure in the microchannel (generally less than 5% of the latter), thus it was reasonable to assume an incompressible fluid flow.

Sometimes fluid flow in small microchannels will exhibit rarefaction effects. For gaseous flow, significant slip flow behavior will occur when Knudsen number (the ratio of mean free path to hydraulic diameter) is larger than 0.001 [38]. However, for the present test, the mean free path of N_2 at ambient condition was considered to be 67.6 nm [39], therefore in our two micromixers (D_H = 528 and 333 μm), the N_2 Knudsen numbers were about 0.00013 and 0.0002, respectively. Consequently, rarefaction effects were negligible. For liquid flow, slip flow is more difficult to occur [27]. In a word, the occurrence of slip flow behavior in the present test was excluded and the classic Navier–Stokes equation with non-slip flow boundary conditions is still applicable.

As clearly demonstrated in recent papers [23,24,26], a detailed experimental uncertainty analysis and additional measurement cautions should be considered prior to the reasonable interpretation of experimental results.

Thus, to eliminate entrance and exit effects, the pressure drop was measured on board some distance from the inlet and outlet, i.e., between ports 2 and 3 in Fig. 1 and the experiments were performed under the condition that the calculated entrance length was lower than the distance between ports 1 and 2 to ensure fully developed laminar flow in the test section. The following equation for entrance

length calculation is used [40]:

$$L_e = 0.09ReD_H \quad (1)$$

Also, a careful experimental uncertainty analysis must be performed. Therefore, for a rectangular microchannel built in the T-type micromixer, we have

$$Re = \frac{2\rho Q}{\mu(H+W)} \quad (2)$$

$$f = \frac{4\Delta p H^3 W^3}{\rho \Delta L Q^2 (H+W)} \quad (3)$$

$$fRe = \frac{8\Delta p H^3 W^3}{Q\Delta L \mu (H+W)^2} \quad (4)$$

According to error analysis theory, the uncertainties in *Re*, *f* and *fRe* are estimated as follows [41]:

$$\frac{\delta Re}{Re} = \left[\left(\frac{\delta Q}{Q}\right)^2 + \left(\frac{\delta\rho}{\rho}\right)^2 + \left(\frac{\delta\mu}{\mu}\right)^2 + \left(\frac{\delta H + \delta W}{H+W}\right)^2\right]^{1/2} \quad (5)$$

$$\frac{\delta f}{f} = \left[\left(\frac{\delta\Delta p}{\Delta p}\right)^2 + \left(\frac{\delta\rho}{\rho}\right)^2 + \left(2\frac{\delta Q}{Q}\right)^2 + \left(\frac{\delta\Delta L}{\Delta L}\right)^2 + \left(3\frac{\delta H}{H}\right)^2 + \left(3\frac{\delta W}{W}\right)^2 + \left(\frac{\delta H + \delta W}{H+W}\right)^2\right]^{1/2} \quad (6)$$

$$\frac{\delta fRe}{fRe} = \left[\left(\frac{\delta\Delta p}{\Delta p}\right)^2 + \left(\frac{\delta Q}{Q}\right)^2 + \left(\frac{\delta\Delta L}{\Delta L}\right)^2 + \left(\frac{\delta\mu}{\mu}\right)^2 + \left(3\frac{\delta H}{H}\right)^2 + \left(3\frac{\delta W}{W}\right)^2 + \left(2\frac{\delta H + \delta W}{H+W}\right)^2\right]^{1/2} \quad (7)$$

The derivation of experimental errors in the parameters located in the right sides of Eqs. (5)–(7) is demonstrated in Table 3 and it should be claimed here that these estimations are rather conservative because most uncertainties in basic measured parameters (*H*, *W*, ΔL, etc.) were taken to be at the minimum level. The uncertainties in the density and viscosity of fluids depend on the measurement accuracies of temperature, pressure and the correlations to describe them, therefore their uncertainties were assumed to be about 1% in this paper. Meanwhile, Eqs. (5)–(7) suggest that in determining *fRe* and *f* for fluid laminar flow in microchannels, the measurement error in the microchannel size contributes to the overall experimental uncertainty most due to the highest factors by which $\delta H/H$, $\delta W/W$ and $(\delta H + \delta W)/(H + W)$ *W* are multiplied.

Using the estimated errors of parameters listed in Table 3, it was found that the conservative experimental uncertainties in *fRe*, *f* and *Re* are 13.58, 13.14 and 3.74% for the micromixer with 528 μm hydraulic diameter respectively, and 21.30, 20.11 and 5.13% for the micromixer with 333 μm hydraulic diameter, respectively.

According to classic theory, the friction constant for single-phase isothermal, incompressible and fully developed laminar flow in a rectangular channel, i.e., the product of friction factor and Reynolds number is [40]:

$$fRe = 96(1 - 3.5553\alpha + 1.9467\alpha^2 - 1.7012\alpha^3 + 0.9564\alpha^4 - 0.2537\alpha^5) \quad (8)$$

where

$$\alpha = \frac{H}{W} \quad (9)$$

As indicated in Figs. 5 and 6, in microchannels of the two micromixers, the experimentally derived friction factor is a function of Reynolds number for N_2 and water laminar flows respectively. The line $f = C/Re$, predicted by classic theory, is also plotted for comparison ($C = 57.3$ for $D_H = 528\,\mu m$ microchannel and $C = 56.9$ for $D_H = 333\,\mu m$ microchannel). Considering the measurement uncertainties, measured *f* is in good agreement with the classic theory predictions under the present laminar flow conditions.

Another method clearly demonstrating fluid laminar flow behavior is to plot figures showing friction constant as a function of Reynolds number, as displayed in Figs. 7 and 8. Obviously, the measured *fRe* values are nearly independent of *Re* given the small differences from the classic *fRe* values within the experiment uncertainties.

Consequently, we can conclude that in fully developed, incompressible and isothermal laminar flow region, fluid behavior in microchannels with diameters of several hundred micrometers still obeys classic theory, which is also proved by many other authors [19–25]. Even if such micro effects as electro-viscous effects for liquid flow and roughness effects exist [8–16], they only play minor roles in determining the friction factor of fluid flow in the smooth or near smooth microchannels used in this work. In other words, without excluding the experiment uncertainties, the influences of these effects are hard to recognize.

Table 3
Experimental errors in parameters located in the right sides of Eqs. (5)–(7)

Parameter	δH (μm)	δW (μm)	$\delta\Delta L$ (μm)	$\delta\Delta p/\Delta p$	$\delta\rho/\rho$	$\delta Q/Q$	$\delta\mu/\mu$	$\delta H/H$		$\delta W/W$		$\delta\Delta L/\Delta L$
								$D_H = 528\,\mu m$, $H = 488\,\mu m$	$D_H = 333\,\mu m$, $H = 332\,\mu m$	$D_H = 528\,\mu m$, $W = 575\,\mu m$	$D_H = 333\,\mu m$, $W = 333\,\mu m$	$\Delta L \approx 3.5\,cm$
Experimental error	~15	~15	~20	~1%	~1%	~2%	~1%	~3.08%	~4.52%	~2.61%	~4.50%	~0.06%

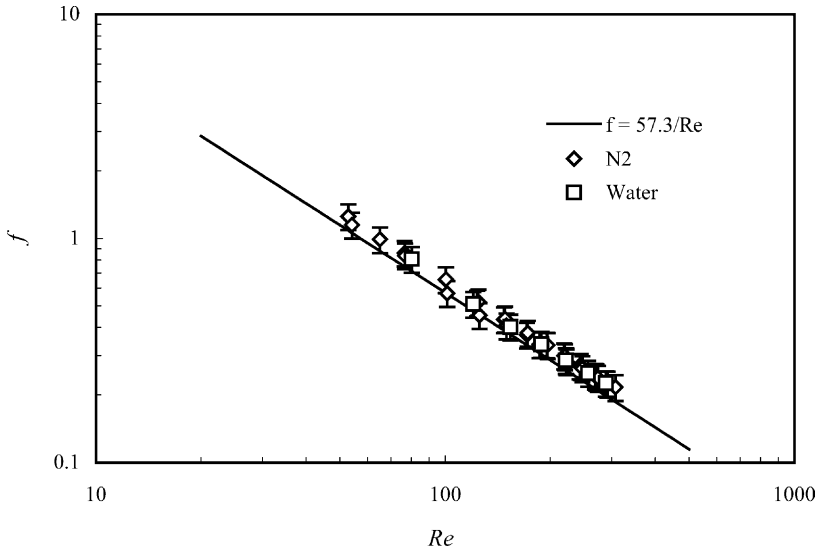

Fig. 5. Friction factor for fluid flow in the microchannel with hydraulic diameter of 528 μm.

3.2. Two-phase flow

3.2.1. Analysis of pressure drop data

For horizontal two-phase flow, the measured total pressure drop is expressed as

$$\Delta p_{\mathrm{T}} = \Delta p_{\mathrm{F}} + \Delta p_{\mathrm{A}} \tag{10}$$

where

$$\Delta p_{\mathrm{A}} = G^2 \left[\left(\frac{x^2}{\rho_{\mathrm{G}}\alpha} + \frac{(1-x)^2}{(1-\alpha)\rho_{\mathrm{L}}} \right)_{\mathrm{outlet}} - \left(\frac{x^2}{\rho_{\mathrm{G}}\alpha} + \frac{(1-x)^2}{(1-\alpha)\rho_{\mathrm{L}}} \right)_{\mathrm{inlet}} \right] \tag{11}$$

Apparently, void fraction data are needed for the calculation of the acceleration pressure drop. According to the classification by Akbar et al. [31], the two-phase flow patterns under our experimental conditions (for the microchannel with $D_{\mathrm{H}} = 528\,\mu\mathrm{m}$, $We_{\mathrm{LS}} = 0.24$–5.94, $We_{\mathrm{GS}} = 0.020$–7.19; for the microchannel with $D_{\mathrm{H}} = 333\,\mu\mathrm{m}$, $We_{\mathrm{LS}} = 0.97$–5.25, $We_{\mathrm{GS}} = 0.030$–8.22) might cover slug flow regime and transitional zone, as evidenced in the experiments at the lowest gas flow rate where slug flow was clearly observed. Consequently the classic drift flux model was chosen to roughly describe the void fractions in microchannels. It means

$$j_{\mathrm{G}}/\alpha = C_0 j + V_b \tag{12}$$

For a horizontal flow [42], $V_b = 0$ and $C_0 = 1.2$ were assumed and Eq. (12) can be further reduced to

$$\alpha = 0.833\beta \tag{13}$$

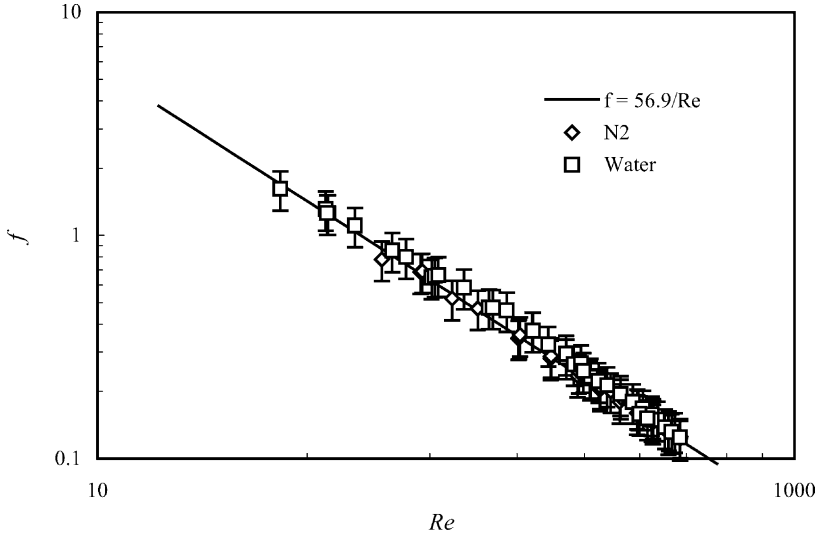

Fig. 6. Friction factor for fluid flow in the microchannel with hydraulic diameter of 333 μm.

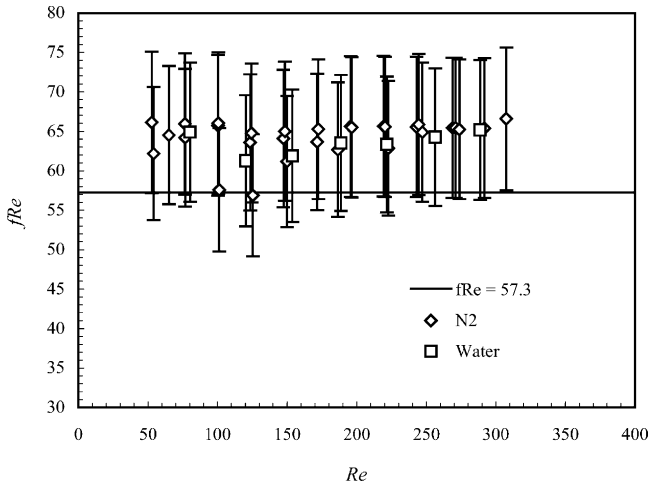

Fig. 7. Friction constant for fluid flow in the microchannel with hydraulic diameter of 528 μm.

where

$$\beta = j_G/j \tag{14}$$

Eq. (13) is in reasonable agreement with those described by Serizawa et al. [29] and Zhao and Bi [32].

Figs. 9 and 10 present the pressure drop data of N_2–water two-phase flow in the micromixers with hydraulic diameters of 528 and 333 μm, respectively. From these figures it was found that the two-phase total pressure drop increased with increasing j_G for constant j_L, and increased with increasing j_L for constant j_G as well. The acceleration pressure drop was only less than 2% of the total pressure drop under the present experimental conditions. Nevertheless, the significant pressure differences in microchannels would cause the density of N_2 to change dramatically along the channel, so the average N_2 density based on the average pressure between two pressure taps was used in correlating frictional pressure drop data.

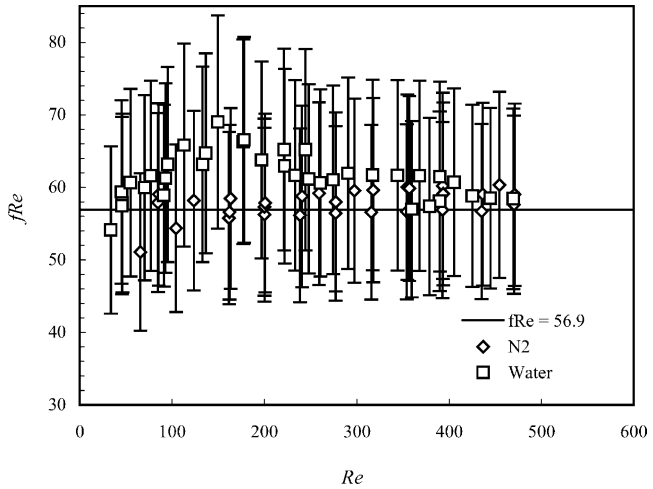

Fig. 8. Friction constant for fluid flow in the microchannel with hydraulic diameter of 333 μm.

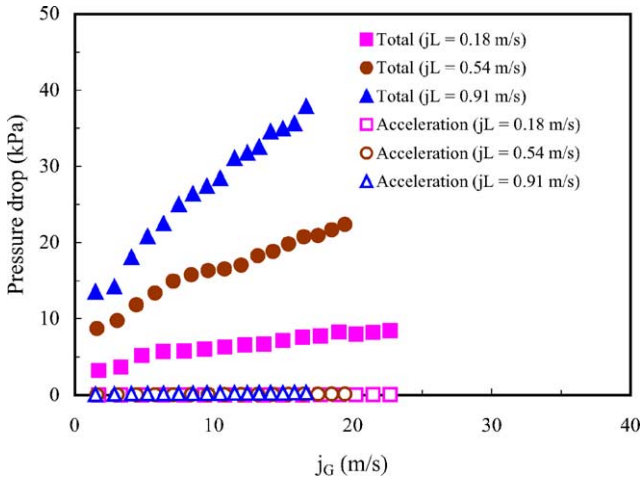

Fig. 9. Total and acceleration pressure drop data of two-phase flow in the micromixer with hydraulic diameter of 528 μm.

3.2.2. Comparisons with existing flow pattern-independent models

Flow pattern-independent models are widely used in calculating two-phase pressure drop for engineering applications, which is mainly due to their simplicities without necessity to know the details of two-phase flow. Among them, separated flow model and homogeneous flow model are well known and used by many people [42]. Therefore, based on the measured data, the adequacy of predictions based on these two models for the interpretation of two-phase pressure drop characteristics in T-type micromixers will be examined here.

A generally accepted correlation to describe two-phase frictional pressure drop based on a separated flow assumption was proposed by Lockhart and Martinelli [43]. It suggests that

$$\left(\frac{\Delta p_F}{\Delta L}\right)_{TP} = \Phi_L^2 \left(\frac{\Delta p_F}{\Delta L}\right)_L \tag{15}$$

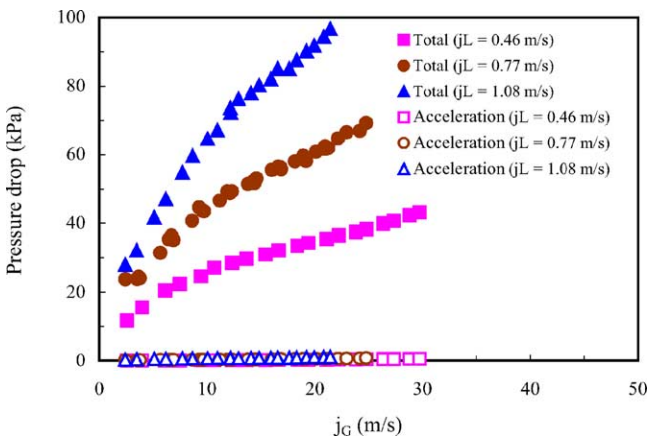

Fig. 10. Total and acceleration pressure drop data of two-phase flow in the micromixer with hydraulic diameter of 333 μm.

Table 4
C values in Eq. (17) for different types of flow

Gas flow regime	Liquid flow regime	C
Laminar	Laminar	5
Laminar	Turbulent	10
Turbulent	Laminar	12
Turbulent	Turbulent	20

$$X^2 = \frac{(\Delta p_F/\Delta L)_L}{(\Delta p_F/\Delta L)_G} \tag{16}$$

where $(\Delta p_F/\Delta L)_{TP}$ is the two-phase frictional pressure drop gradient while $(\Delta p_F/\Delta L)_L$ and $(\Delta p_F/\Delta L)_G$ represent the frictional pressure drop gradient when liquid and gas are assumed to flow in the microchannel alone, respectively. Based on the single-phase flow results described in Section 3.1, $(\Delta p_F/\Delta L)_L$ and $(\Delta p_F/\Delta L)_G$ can be calculated using classic laminar flow theory under the testing conditions of the two-phase flow.

Lockhart and Martinelli [43] only presented the curve of Φ_L^2 versus X. Later Chisholm [44] proposed the following equation to correlate the relationship between them, that is

$$\Phi_L^2 = 1 + \frac{C}{X} + \frac{1}{X^2} \tag{17}$$

where the value of coefficient C depended on the flow condition of each phase in channels and is listed in Table 4.

Figs. 11 and 12 compare the experimental Φ_L^2 as a function of X with the value predicted by Eq. (17). Because most of the present experiments were conducted under the condition that both Re_{LS} and Re_{GS} were lower than 1000, C value in Eq. (17) should be 5 according to Table 4. However, Figs. 11 and 12 show that for both 528 and 333 μm hydraulic diameter microchannels the experimentally derived C values lie between 5 and 20, implying that Lockhart and Martinelli correlation significantly under-predicts the experimental frictional pressure drop. The deviation far exceeds any possible experimental uncertainties. Similar conclusion was also drawn by Fukano and Kariyasaki [37] who found that frictional multiplier became very large compared to the predictions by the Chisholm's equation in the range of X = 1–10 for air–water two-phase flow in 2.4 mm diameter capillary. They ascribed it to the effect caused by the peculiar flow field of slug flow in small capillaries.

Another deviation is seen from these figures that Lockhart and Martinelli correlation fails to describe the dependence of C value on X and j_L, i.e., the present N_2–water two-phase flow in microchannels exhibits significant mass flux effect, as already proved by other authors for air–water two-phase flow in mini rectangular channels [36,45] and for two-phase flow of refrigerants in a mini tube [46]. Thus a modification of C value in Eq. (17) was developed for the present experiments:

$$C = aX^b Re_{LO}^c \tag{18}$$

where a = 0.411822, b = −0.0305 and c = 0.600428, obtained by a least square regression. Fig. 13 illustrates the good curve fitting performance for this regression.

Figs. 14 and 15 demonstrate the relationships between the experimental Φ_L^2 values and the values predicted by combining Eqs. (17) and (18) for the two micromixers. The agreement between the experimental and theoretical values

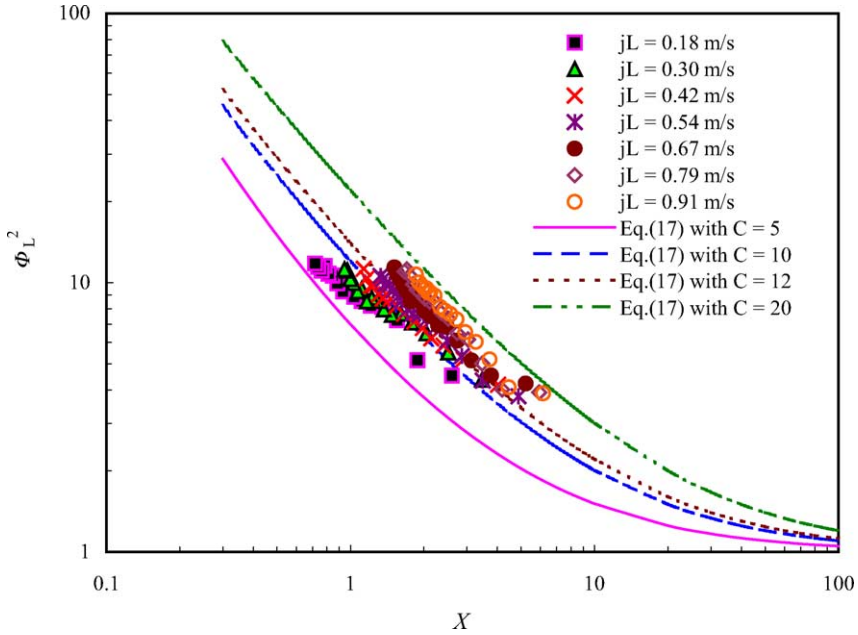

Fig. 11. Relationship between two-phase frictional multiplier and Martinelli parameter for the micromixer with D_H = 528 μm (65 < Re_{GS} < 1000, 99 < Re_{LS} < 504).

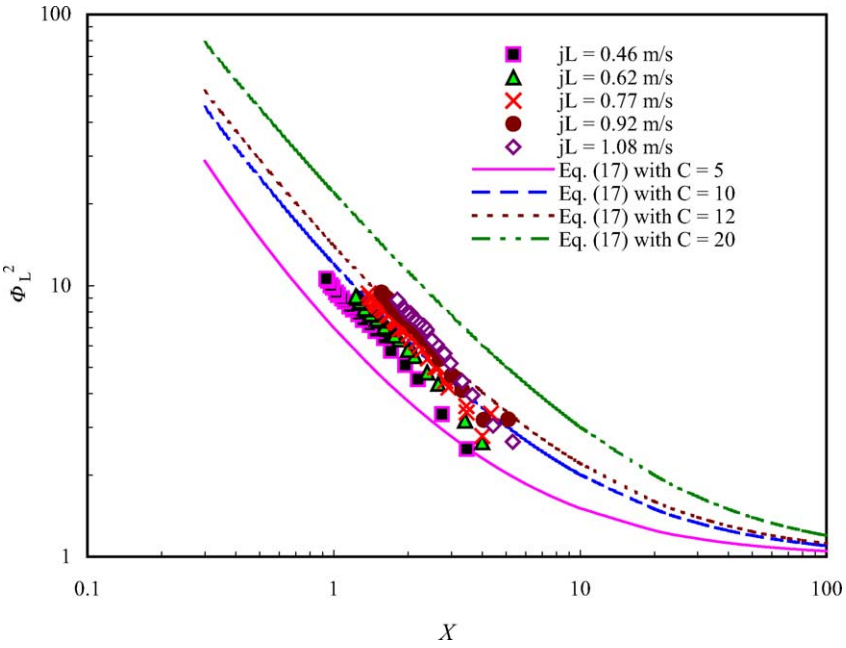

Fig. 12. Relationship between two-phase frictional multiplier and Martinelli parameter for the micromixer with $D_H = 333\,\mu m$ ($66 < Re_{GS} < 1000$, $134 < Re_{LS} < 330$).

is satisfactory for either of the two mixers. If the mean deviation is given by

$$\frac{\sum_{i=1}^{N} |(\text{the } i\text{th predicted value} - \text{the } i\text{th measured value})/\text{the } i\text{th measured value}|}{N} \times 100\%,$$

then the Φ_L^2 mean deviations for micromixers with $D_H = 528$ and $333\,\mu m$ are 6.35 and 6.29%, respectively. The percentage of Φ_L^2 data lying within the error bound of ±20% is 95.5 and 93.8% for the respective micromixer.

In contrast to the separated flow model, the homogeneous flow model treats two-phase mixture as a well-mixed pseudo-single-phase fluid with homogeneous mixture density and viscosity. Generally speaking, in the homogenous flow model, we have

$$\left(\frac{\Delta p_F}{\Delta L}\right)_{TP} = f\frac{1}{D_H}\frac{G^2}{2\rho_{TP}} \tag{19}$$

where under laminar flow condition

$$\frac{1}{\rho_{TP}} = \frac{x}{\rho_G} + \frac{1-x}{\rho_L} \tag{20}$$

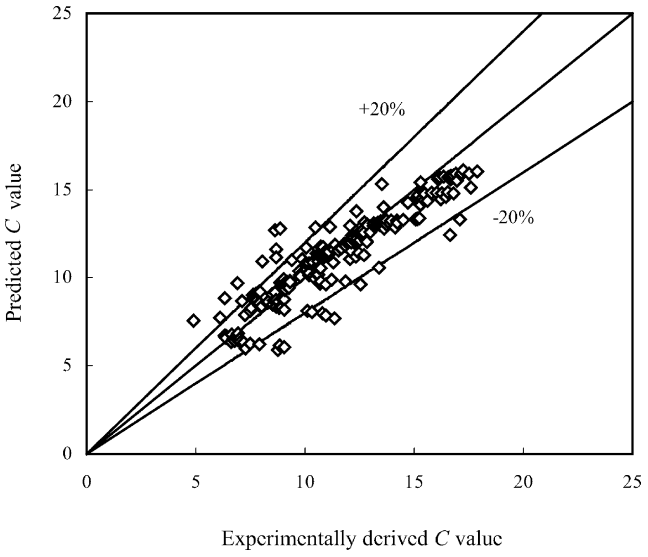

Fig. 13. Performance of Eq. (18) in predicting C value in the Chisholm's equation.

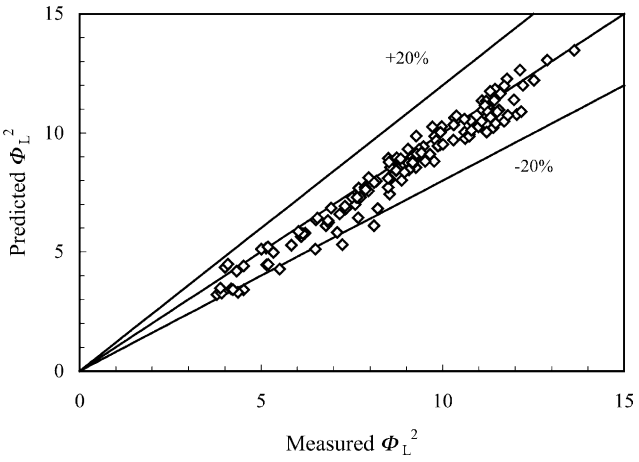

Fig. 14. Comparison of measured Φ_L^2 to that predicted by combining Eqs. (17) and (18) for the micromixer with $D_H = 528\,\mu m$.

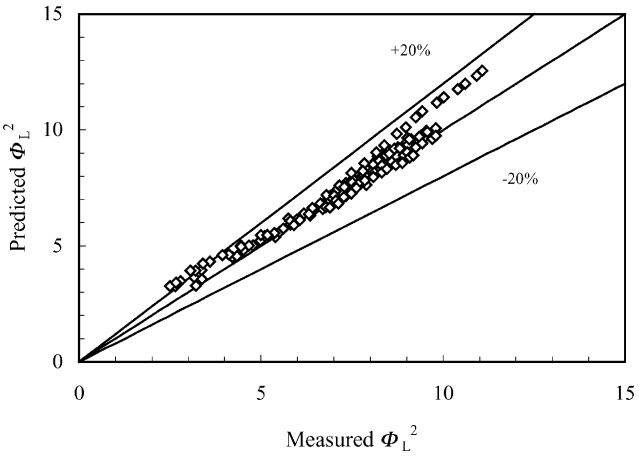

Fig. 15. Comparison of measured Φ_L^2 to that predicted by combining Eqs. (17) and (18) for the micromixer with $D_H = 333\,\mu m$.

$$f = \frac{C}{Re_{TP}} \tag{21}$$

$$Re_{TP} = \frac{GD_H}{\mu_{TP}} \tag{22}$$

Therefore, how to choose a reasonable and proper mixture viscosity from the many available homogeneous viscosity correlations [42,47,48] is crucial to a successful interpretation of the two-phase frictional pressure drop data. As we found that fluid laminar flow in the present microchannels generally obeys classic theory, the selection of viscosity correlations was limited to those that would cause the homogeneous Reynolds number, Re_{TP}, under the present experimental conditions lower than 2000. With this constraint, the available useful viscosity correlations were those by McAdams [42], Owens [42], and Cicchitti et al. [47] and Lin et al. [48]. The corresponding equations are given in Table 5.

Figs. 16 and 17 present the comparisons between the experimental frictional pressure drop gradient data with the predictions using models listed in Table 5. Their overall performances were also evaluated in Table 5. It is obvious that all relevant correlations except that of McAdams over-predict the two-phase flow frictional pressure drop as a whole and the latter provides the least deviation: 76.7% of the predictions lie in the error bound of ±30% for the micromixer with $D_H = 528\,\mu m$ and 82.2% for the micromixer with $D_H = 333\,\mu m$. This conclusion was found to agree with that of Triplett et al. [35] who had reported that homogeneous flow model based on McAdams mixture

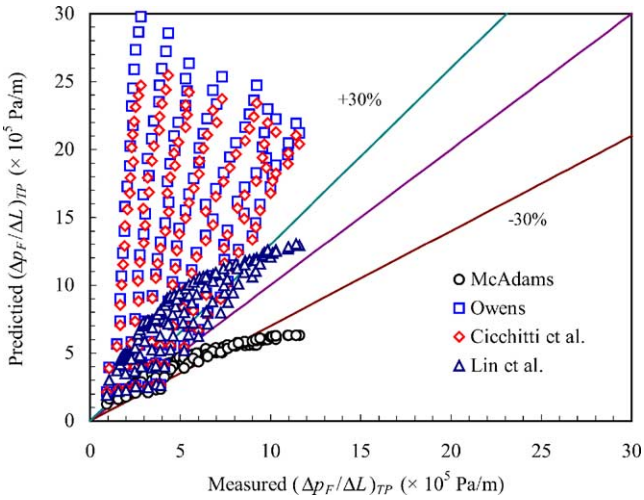

Fig. 16. Comparison between measured frictional pressure drop gradient data and predictions based on homogeneous flow models for the micromixer with $D_H = 528\,\mu m$.

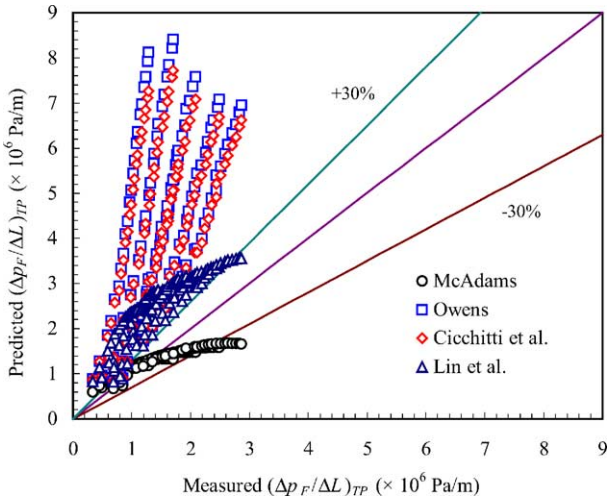

Fig. 17. Comparison between measured frictional pressure drop gradient data and predictions based on homogeneous flow models for the micromixer with $D_H = 333\,\mu m$.

Table 5
Viscosity correlations and corresponding performances in predicting two-phase flow frictional pressure drop in microchannels

Viscosity model	Equation (number)		$D_H = 528\,\mu m$		$D_H = 333\,\mu m$	
			Re_{TP}	Mean deviation (%)	Re_{TP}	Mean deviation (%)
McAdams [42]	$\mu_{TP} = \left(\frac{x}{\mu_G} + \frac{1-x}{\mu_L}\right)^{-1}$	(23)	153–1601	19.31	201–1394	18.15
Owens [42]	$\mu_{TP} = \mu_L$	(24)	88–461	244.38	136–334	201.92
Cicchitti et al. [47]	$\mu_{TP} = x\mu_G + (1-x)\mu_L$	(25)	89–480	221.14	136–351	187.96
Lin et al. [48]	$\mu_{TP} = \frac{\mu_G\mu_L}{\mu_G + x^{1.4}(\mu_L - \mu_G)}$	(26)	99–776	67.54	145–652	76.91

viscosity also predicted their pressure drop of air–water bubbly flow and slug flow in microchannels well.

4. Conclusions

Experiments were performed on pressure drops of fluid (N_2, water) single-phase flow and N_2–water two-phase flow in microchannels built in T-type micromixers of two different sizes ($D_H = 528$ and $333\,\mu m$, respectively). The following conclusions are deduced here:

(1) Fluid laminar flow in smooth or near smooth microchannels with hydraulic diameters of several hundred micrometers obeys classic theory. And if there exist such micro effects as electro-viscous effects for liquid flow, roughness effects, their impacts are negligible in such microchannels or at least cannot be identified with the consideration of the experimental uncertainties.

(2) For N_2–water two-phase flow in microchannel mixers with hydraulic diameters of several hundred micrometers, generally the separated flow model and homogeneous flow model cannot predict the frictional pressure drop well. Among the homogeneous mixture assumptions investigated, the viscosity correlation of McAdams provides the best predictions for the experimental data.

(3) A modification of C value in the Chisholm's equation used for Lockhart and Martinelli correlation accounting for mass flux effect was developed:

$$C = 0.411822 X^{-0.0305} Re_{LO}^{0.600428} \quad (27)$$

It was found that this modification could describe the present experimental data well ($Re_{LO} = 88$–461, $X = 0.67$–6.16).

(4) Since most interpretations of available results about two-phase pressure drop characteristics in microchannels are still based on traditional empirical or semi-empirical correlations and generally the agreements are poor, there is a need to conduct systematic studies addressing the coupling between the underlying mechanism of two-phase flow and macroscopic pressure drop characteristics, which was also the attempts of Fukano and Kariyasaki [37] and Garimella et al. [49]. By this effort, we may take the full advantage of microchannels in heat transfer and chemical reaction applications.

Acknowledgements

We gratefully acknowledge the financial supports for this project from National Natural Science Foundation of China (No. 20176057 and No. 20376080), National Fundamental Research Development Program of China (No. 2000026401) and Key Program for International Cooperation of Science and Technology (No. 2001CB711203), and Innovative Fund of Dalian Institute of Chemical Physics, Chinese Academy of Sciences (No. K2003E09030408).

References

[1] W. Ehrfeld, K. Golbig, V. Hessel, H. Lowe, T. Richter, Characterization of mixing in micromixers by a test reaction: Single mixing units and mixer arrays, Ind. Eng. Chem. Res. 38 (1999) 1075–1082.

[2] K.F. Jensen, Microreaction engineering—is small better, Chem. Eng. Sci. 56 (2001) 293–303.

[3] M.W. Losey, M.A. Schmidt, K.F. Jensen, Microfabricated multiphase packed-bed reactors: Characterization of mass transfer and reactions, Ind. Eng. Chem. Res. 40 (2001) 2555–2562.

[4] K. Jahnisch, M. Baerns, V. Hessel, W. Ehrfeld, V. Haverkamp, H. Lowe, C. Wille, A. Guber, Direct fluorination of toluene using elemental fluorine in gas/liquid microreactors, J. Fluorine Chem. 105 (2000) 117–128.

[5] N. de Mas, A. Gunther, M.A. Schmidt, K.F. Jensen, Microfabricated multiphase reactors for the selective direct fluorination of aromatics, Ind. Eng. Chem. Res. 42 (2003) 698–710.

[6] T.M. Harms, M.J. Kazmierczak, F.M. Gerner, Developing convective heat transfer in deep rectangular microchannels, Int. J. Heat Fluid Flow 20 (1999) 149–157.

[7] W.L. Qu, I. Mudawar, Measurement and prediction of pressure drop in two-phase micro-channel heat sinks, Int. J. Heat Mass Transfer 46 (2003) 2737–2753.

[8] P.Y. Wu, W.A. Little, Measurement of friction factors for the flow of gases in very fine channels used for microminiature Joule-Thomson refrigerators, Cryogenics 23 (1983) 273–277.

[9] I. Papautsky, J. Brazzle, T. Ameel, A.B. Frazier, Laminar fluid behavior in microchannels using micropolar fluid theory, Sens. Actuators A 73 (1999) 101–108.

[10] D. Pfund, D. Rector, A. Shekarriz, A. Popescu, J. Welty, Pressure drop measurements in a microchannel, AICHE J. 46 (2000) 1496–1507.

[11] L.Q. Ren, W.L. Qu, D.Q. Li, Interfacial electrokinetic effects on liquid flow in microchannels, Int. J. Heat Mass Transfer 44 (2001) 3125–3134.

[12] G.M. Mala, D.Q. Li, C. Werner, H.J. Jacobasch, Y.B. Ning, Flow characteristics of water through a microchannel between two parallel plates with electrokinetic effects, Int. J. Heat Fluid Flow 18 (1997) 489–496.

[13] C. Yang, D.Q. Li, J.H. Masliyah, Modeling forced liquid convection in rectangular microchannels with electrokinetic effects, Int. J. Heat Mass Transfer 41 (1998) 4229–4249.

[14] L.Q. Ren, D.Q. Li, W.L. Qu, Electro-viscous effects on liquid flow in microchannels, J. Colloid Interface Sci. 233 (2001) 12–22.

[15] G.M. Mala, D.Q. Li, Flow characteristics of water in microtubes, Int. J. Heat Fluid Flow 20 (1999) 142–148.

[16] W.L. Qu, G.M. Mala, D.Q. Li, Pressure-driven water flows in trapezoidal silicon microchannels, Int. J. Heat Mass Transfer 43 (2000) 353–364.

[17] D. Yu, R. Warrington, R. Barron, T. Ameel, Experimental and theoretical investigation of fluid flow and heat transfer in microtubes, in: Proceedings of the ASME-JSME Thermal Engineering Joint Conference, Maui, HI, USA, 19–24 March 1995, pp. 523–530.

[18] X.N. Jiang, Z.Y. Zhou, X.Y. Huang, C.Y. Liu, Laminar flow through microchannels used for microscale cooling systems, in: Proceedings of IEEE/CPMT Electronic Packaging Technology Conference, 1997, pp.119–122.

[19] S.M. Flockhart, R.S. Dhariwal, Experimental and numerical investigation into the flow characteristics of channels etched in <100> silicon, J. Fluids Eng. 120 (1998) 291–295.
[20] K.V. Sharp, R.J. Adrian, D.J. Beebe, Anomalous transition to turbulence in microtubes, in: Proceedings of 2000 ASME International Mechanical Engineering Congress and Exposition, Orlando, FL, 5–10 November 2000, pp. 461–466.
[21] B. Xu, K.T. Ooi, N.T. Wong, W.K. Choi, Experimental investigation of flow friction for liquid flow in microchannels, Int. Commun. Heat Mass Transfer 27 (2000) 1165–1176.
[22] H.H. Bau, J.N. Pfahler, Experimental observations of liquid flow in micro conduits, in: Proceedings of 39th AIAA Aerospace Sciences Meeting & Exhibit, Reno, NV, 8–11 January 2001, AIAA paper 2001-0722.
[23] J. Judy, D. Maynes, B.W. Webb, Characterization of frictional pressure drop for liquid flows through microchannels, Int. J. Heat Mass Transfer 45 (2002) 3477–3489.
[24] D. Liu, S.V. Garimella, Investigation of liquid flow in microchannels, in: Proceedings of Eighth AIAA/ASME Joint Thermophysics and Heat Transfer Conference, St. Louis, Missouri, 24–26 June 2002, AIAA paper 2002-2776.
[25] H.Y. Wu, P. Cheng, Friction factors in smooth trapezoidal silicon microchannels with different aspect ratios, Int. J. Heat Mass Transfer 46 (2003) 2519–2525.
[26] I. Papautsky, T. Ameel, A.B. Frazier, A review of laminar single-phase flow in microchannels, in: Proceedings of 2001 ASME International Mechanical Engineering Congress and Exposition, New York, 11–16 November 2001, pp. 495–503.
[27] J. Koo, C. Kleinstreuer, Liquid flow in microchannels: experimental observations and computational analyses of microfluidics effects, J. Micromech. Microeng. 13 (2003) 568–579.
[28] T.S. Zhao, Q.C. Bi, Co-current air–water two-phase flow patterns in vertical triangular microchannels, Int. J. Multiphase Flow 27 (2001) 765–782.
[29] A. Serizawa, Z.P. Feng, Z. Kawara, Two-phase flow in microchannels, Exp. Therm. Fluid Sci. 26 (2002) 703–714.
[30] A. Kawahara, P.M.Y. Chung, M. Kawaji, Investigation of two-phase flow pattern void fraction and pressure drop in a microchannel, Int. J. Multiphase Flow 28 (2002) 1411–1435.
[31] M.K. Akbar, D.A. Plummer, S.M. Ghiaasiaan, On gas-liquid two-phase flow regimes in microchannels, Int. J. Multiphase Flow 29 (2003) 855–865.
[32] T.S. Zhao, Q.C. Bi, Pressure drop characteristics of gas-liquid two-phase flow in vertical miniature triangular channels, Int. J. Heat Mass Transfer 44 (2001) 2523–2534.
[33] W.L. Chen, M.C. Twu, C. Pan, Gas-liquid two-phase flow in micro-channels, Int. J. Multiphase Flow 28 (2002) 1235–1247.
[34] K.A. Triplett, S.M. Ghiaasiaan, S.I. Abdel-Khalik, D.L. Sadowski, Gas-liquid two-phase flow in microchannels – Part I: two-phase flow patterns, Int. J. Multiphase Flow 25 (1999) 377–394.
[35] K.A. Triplett, S.M. Ghiaasiaan, S.I. Abdel-Khalik, A. LeMouel, B.N. McCord, Gas-liquid two-phase flow in microchannels – Part II: void fraction and pressure drop, Int. J. Multiphase Flow 25 (1999) 395–410.
[36] M.I. Ali, M. Sadatomi, M. Kawaji, Adiabatic two-phase flow in narrow channels between two flat plates, Can. J. Chem. Eng. 71 (1993) 657–666.
[37] T. Fukano, A. Kariyasaki, Characteristics of gas-liquid two-phase flow in a capillary-tube, Nucl. Eng. Des. 141 (1993) 59–68.
[38] M. Gad-el-Hak, Use of continuum and molecular approaches in microfluidics, in: Proceedings of the Third Theoretical Fluid Mechanics Meeting, St. Louis, Missouri, 24–26 June 2002, AIAA paper 2002-2868.
[39] D.R. Lide (Ed.), CRC Handbook of Chemistry and Physics 1999–2000, 80th ed., CRC Press LLC, Boca raton, 1999, pp. 6–46.
[40] R.K. Shah, A.L. London, Laminar Flow Forced Convection in Ducts, Academic Press, New York, 1978.
[41] R.J. Moffat, Describing the uncertainties in experimental results, Exp. Therm. Fluid Sci. 1 (1988) 3–17.
[42] G.B. Wallis, One Dimensional Two-phase Flow, McGraw-Hill, New York, 1969.
[43] R.W. Lockhart, R.C. Martinelli, Proposed correlation of data for isothermal two-phase, two-component flow in pipes, Chem. Eng. Prog. 45 (1949) 39–48.
[44] D. Chisholm, A Theoretical basis for the Lockhart–Martinelli correlation for two-phase flow, Int. J. Heat Mass Transfer 10 (1967) 1767–1778.
[45] M.W. Wambsganss, J.A. Jendrzejczyk, D.M. France, N.T. Obot, Frictional pressure-gradients in two-phase flow in a small horizontal rectangular channel, Exp. Therm. Fluid Sci. 5 (1992) 40–56.
[46] C.C. Wang, C.S. Chiang, D.C. Lu, Visual observation of two-phase flow pattern of R-22, R-134a, and R-407C in a 6.5-mm smooth tube, Exp. Therm. Fluid Sci. 15 (1997) 395–405.
[47] T.N. Wong, K.T. Ooi, Refrigerant flow in capillary tube: an assessment of the two-phase viscosity correlations on model prediction, Int. Commun. Heat Mass Transfer 22 (1995) 595–604.
[48] S. Lin, C.C.K. Kwok, R.Y. Li, Z.H. Chen, Z.Y. Chen, Local frictional pressure drop during vaporization for R-12 through capillary tubes, Int. J. Multiphase flow 17 (1991) 95–102.
[49] S. Garimella, J.D. Killion, J.W. Coleman, An experimentally validated model for two-phase pressure drop in the intermittent flow regime for circular microchannels, J. Fluids Eng. 124 (2002) 205–214.